Observation of Direct *CP* Violation in $K_{S,L} \to \pi\pi$ Decays

A. Alavi-Harati,[12] I. F. Albuquerque,[10] T. Alexopoulos,[12] M. Arenton,[11] K. Arisaka,[2] S. Averitte,[10] A. R. Barker,[5] L. Bellantoni,[7] A. Bellavance,[9] J. Belz,[10] R. Ben-David,[7] D. R. Bergman,[10] E. Blucher,[4] G. J. Bock,[7] C. Bown,[4] S. Bright,[4] E. Cheu,[1] S. Childress,[7] R. Coleman,[7] M. D. Corcoran,[9] G. Corti,[11] B. Cox,[11] M. B. Crisler,[7] A. R. Erwin,[12] R. Ford,[7] A. Glazov,[4] A. Golossanov,[11] G. Graham,[4] J. Graham,[4] K. Hagan,[11] E. Halkiadakis,[10] K. Hanagaki,[8] S. Hidaka,[8] Y. B. Hsiung,[7] V. Jejer,[11] J. Jennings,[2] D. A. Jensen,[7] R. Kessler,[4] H. G. E. Kobrak,[3] J. LaDue,[5] A. Lath,[10] A. Ledovskoy,[11] P. L. McBride,[7] A. P. McManus,[11] P. Mikelsons,[5] E. Monnier,[4,*] T. Nakaya,[7] U. Nauenberg,[5] K. S. Nelson,[11] H. Nguyen,[7] V. O'Dell,[7] M. Pang,[7] R. Pordes,[7] V. Prasad,[4] C. Qiao,[4] B. Quinn,[4] E. J. Ramberg,[7] R. E. Ray,[7] A. Roodman,[4] M. Sadamoto,[8] S. Schnetzer,[10] K. Senyo,[8] P. Shanahan,[7] P. S. Shawhan,[4] W. Slater,[2] N. Solomey,[4] S. V. Somalwar,[10] R. L. Stone,[10] I. Suzuki,[8] E. C. Swallow,[4,6] R. A. Swanson,[3] S. A. Taegar,[1] R. J. Tesarek,[10] G. B. Thomson,[10] P. A. Toale,[5] A. Tripathi,[2] R. Tschirhart,[7] Y. W. Wah,[4] J. Wang,[1] H. B. White,[7] J. Whitmore,[7] B. Winstein,[4] R. Winston,[4] J.-Y. Wu,[5] T. Yamanaka,[8] and E. D. Zimmerman[4]

(KTeV Collaboration)

[1]*University of Arizona, Tucson, Arizona 85721*
[2]*University of California at Los Angeles, Los Angeles, California 90095*
[3]*University of California at San Diego, La Jolla, California 92093*
[4]*The Enrico Fermi Institute, The University of Chicago, Chicago, Illinois 60637*
[5]*University of Colorado, Boulder, Colorado 80309*
[6]*Elmhurst College, Elmhurst, Illinois 60126*
[7]*Fermi National Accelerator Laboratory, Batavia, Illinois 60510*
[8]*Osaka University, Toyonaka, Osaka 560, Japan*
[9]*Rice University, Houston, Texas 77005*
[10]*Rutgers University, Piscataway, New Jersey 08855*
[11]*The Department of Physics and Institute of Nuclear and Particle Physics, University of Virginia, Charlottesville, Virginia 22901*
[12]*University of Wisconsin, Madison, Wisconsin 53706*

(Received 27 May 1999)

We have compared the decay rates of K_L and K_S to $\pi^+\pi^-$ and $\pi^0\pi^0$ final states using a subset of the data from the KTeV experiment (E832) at Fermilab. We find that the direct-*CP*-violation parameter $\mathrm{Re}(\epsilon'/\epsilon)$ is equal to $[28.0 \pm 3.0(\mathrm{stat}) \pm 2.8(\mathrm{syst})] \times 10^{-4}$. This result definitively establishes the existence of *CP* violation in a decay process.

PACS numbers: 13.25.Es, 11.30.Er, 14.40.Aq

The neutral K meson system has been the subject of much study since it was recognized that the two strangeness states (K^0, $\overline{K}^0$) mix to produce short- and long-lived kaons (K_S, K_L). The unexpected discovery of $K_L \to \pi\pi$ decays in 1964 [1] revealed that *CP* (charge-parity) symmetry is violated by the weak interaction, and it was soon understood that the dominant effect is an asymmetry in the K^0-$\overline{K}^0$ mixing, parametrized by ϵ. Ever since, there has been great interest in determining whether *CP* violation also occurs in the $K \to \pi\pi$ decay process itself, an effect referred to as "direct" *CP* violation [2] and parametrized by ϵ'. This would contribute differently to the decay rate for $K_L \to \pi^+\pi^-$ versus $K_L \to \pi^0\pi^0$ (relative to the corresponding K_S decays), and thus would be observable as a nonzero value of

$$\mathrm{Re}(\epsilon'/\epsilon) \approx \frac{1}{6}\left[\frac{\Gamma(K_L \to \pi^+\pi^-)/\Gamma(K_S \to \pi^+\pi^-)}{\Gamma(K_L \to \pi^0\pi^0)/\Gamma(K_S \to \pi^0\pi^0)} - 1\right].$$

The standard Cabibbo-Kobayashi-Maskawa (CKM) model [3] can accommodate *CP* violation in a natural way with a complex phase in the quark mixing matrix. The earliest standard-model calculations of $\mathrm{Re}(\epsilon'/\epsilon)$ [4], which gave values of order $\sim 10^{-3}$–10^{-2}, were done before the top quark mass was known and before the importance of certain diagrams was appreciated. Modern calculations depend sensitively on input parameters and on the method used to estimate the hadronic matrix elements. Most recent estimates have tended toward values near or below 10^{-3}, for example, $(4.6 \pm 3.0) \times 10^{-4}$ [5] and $(8.5 \pm 5.9) \times 10^{-4}$ [6]; however, one group has estimated a larger range of values, $(17^{+14}_{-10}) \times 10^{-4}$ [7]. Alternatively, a "superweak" interaction [8] could produce the observed *CP*-violating mixing but would give $\mathrm{Re}(\epsilon'/\epsilon) = 0$. Therefore, a nonzero value of $\mathrm{Re}(\epsilon'/\epsilon)$

 0031-9007/99/83(1)/22(6)$15.00

rules out the possibility that a superweak interaction is the sole source of *CP* violation.

The two most precise past measurements of $\mathrm{Re}(\epsilon'/\epsilon)$ are in only fair agreement: the Fermilab E731 experiment reported $\mathrm{Re}(\epsilon'/\epsilon) = (7.4 \pm 5.9) \times 10^{-4}$ [9], while CERN NA31 found $\mathrm{Re}(\epsilon'/\epsilon) = (23 \pm 6.5) \times 10^{-4}$ [10]. Because of the importance of definitively establishing the existence of direct *CP* violation and determining its magnitude, new experiments have been undertaken at Fermilab, CERN, and Frascati to measure $\mathrm{Re}(\epsilon'/\epsilon)$ with precisions of $(\sim 1\text{–}2) \times 10^{-4}$.

This Letter reports a new measurement of $\mathrm{Re}(\epsilon'/\epsilon)$ using 23% of the data collected by the KTeV experiment (E832) during the 1996–1997 Fermilab fixed-target run. The KTeV experiment was designed to improve upon the previous generation of experiments and ultimately to have the sensitivity to establish direct *CP* violation in the range of the smaller estimates in [5] and [6]. The experimental technique is the same as in E731 [11], and differs from NA31 in two key ways. First, it uses two kaon beams from a single target to enable the simultaneous collection of K_L and K_S decays in order to be insensitive to the inevitable time variation of beam characteristics and detector inefficiencies. Second, it uses a precision magnetic spectrometer to minimize backgrounds in the $\pi^+\pi^-$ samples and to allow *in situ* calibration of the calorimeter. While the method of producing the K_S beam (by passing a K_L beam through a "regenerator") is also the same as in E731, the KTeV regenerator is made of scintillator and is fully instrumented to reduce the scattered-kaon background to the coherently regenerated signal. A new beam line was constructed for KTeV with much cleaner beam collimation and improved muon sweeping [12]. Finally, the KTeV electromagnetic calorimeter has much higher precision than the E731 calorimeter, permitting more accurate $\pi^0\pi^0$ reconstruction and better background suppression.

Figure 1 shows the two beams (called "regenerator" and "vacuum") in the evacuated decay volume, with the main detector elements located downstream. The regenerator alternates sides between accelerator extractions to minimize the effect of any left-right beam or detector asymmetry. A "movable absorber," far upstream, attenuates the beam incident on the regenerator. To measure the double ratio of decay rates in the expression for $\mathrm{Re}(\epsilon'/\epsilon)$, we must understand the *difference* between the acceptances for K_S versus K_L decays to each $\pi\pi$ final state. Triggering, reconstruction, and event selection are done with identical criteria for decays in either beam, so the only major difference is in the decay vertex distributions, shown in Fig. 2 as a function of Z, the distance from the kaon production target. Therefore, the most crucial requirement for measuring $\mathrm{Re}(\epsilon'/\epsilon)$ with this technique is a precise understanding of the Z dependence of the detector acceptance [13].

In the regenerator beam, the beginning of the decay region is sharply defined by a lead-scintillator module at the downstream end of the regenerator. In the vacuum beam, the acceptance for decays upstream of $Z = 122$ m

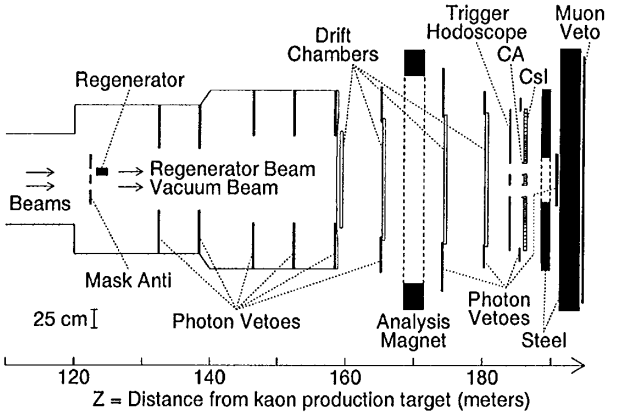

FIG. 1. Plan view of the KTeV apparatus as configured to measure $\mathrm{Re}(\epsilon'/\epsilon)$. The evacuated decay volume ends with a thin vacuum window at $Z = 159$ m. The label "CsI" indicates the electromagnetic calorimeter.

is limited by the "mask anti" (MA), a lead-scintillator counter with two square holes 50% larger than the beams.

The KTeV spectrometer consists of four rectangular drift chambers, each with two horizontal and two vertical planes of sense wires, and a large dipole magnet which imparts a transverse momentum of 0.412 GeV/c. The spaces between the drift chambers are filled with helium to reduce scattering. The drift chambers measure horizontal and vertical track position with a typical resolution of 110 μm and momentum with a resolution of 0.4% at the mean pion momentum of 36 GeV/c.

The electromagnetic calorimeter [14] consists of 3100 blocks of pure cesium iodide (CsI) in a square array 1.9 m on a side and 0.5 m deep. Two 15 cm square beam holes allow passage of the neutral beams through the calorimeter. The calorimeter was calibrated using 1.9×10^8 momentum-analyzed electrons from $K_L \to \pi e \nu$ decays collected during normal running. Individually tuned wrapping of the CsI blocks and the development of very-low-noise readout electronics [15] have enabled the calorimeter to achieve an average energy resolution of 0.7% for photons from $\pi^0\pi^0$ decays, which have a mean energy of 19 GeV.

The inner aperture for photons at the CsI is sharply defined by a tungsten-scintillator "collar anti" (CA) counter

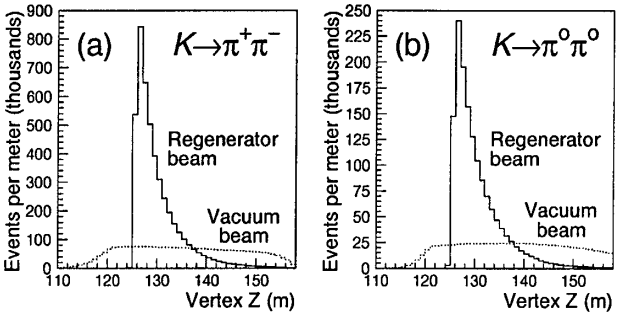

FIG. 2. Decay vertex distributions for the (a) $K \to \pi^+\pi^-$ and (b) $K \to \pi^0\pi^0$ decay modes, showing the difference between the "regenerator" (K_S) and "vacuum" (K_L) beams.

around each beam hole. In addition, there are ten lead-scintillator "photon veto" counters to detect particles escaping from the decay volume or missing the CsI, in order to suppress $K_L \to 3\pi^0$ background in the $\pi^0\pi^0$ samples.

The trigger system initiates detector readout based on synchronous signals from a scintillator hodoscope located upstream of the calorimeter (for $\pi^+\pi^-$) or on a fast analog energy sum from the calorimeter (for $\pi^0\pi^0$). To keep the trigger rate at a manageable level, triggers are inhibited by fast veto signals from the regenerator, the MA, a subset of the photon vetoes, and a downstream hodoscope located behind 4 m of steel to detect muons [16]. For $\pi^+\pi^-$, additional requirements are made on the number and pattern of hits in the drift chambers. For $\pi^0\pi^0$, a hardware processor [17] must find 4 or 5 "clusters" of energy in the calorimeter. After readout, a CPU-based "level 3 filter" reconstructs events and applies some loose kinematic cuts to select $\pi^+\pi^-$ and $\pi^0\pi^0$ candidates. Besides these signal modes, large samples of $K_L \to \pi e \nu$, $K_L \to \pi^+\pi^-\pi^0$, and $K_L \to 3\pi^0$ decays are recorded for detector calibration and acceptance studies. In addition, an "accidental" trigger is formed, using scintillation counters near the kaon production target, to randomly record the underlying activity in the KTeV detector with the same instantaneous-intensity distribution as the physics data.

The $\pi^0\pi^0$ samples used for this analysis are from the data collected in 1996, while the $\pi^+\pi^-$ samples are from the first 18 days of data collected in 1997. We decided not to use the $\pi^+\pi^-$ data from 1996 because the level 3 filter had a 22% inefficiency arising from an unanticipated drift chamber effect which sometimes delayed a hit by 20 ns or more. The inefficiency was nearly the same for both beams but still would have led to a large systematic error on $\mathrm{Re}(\epsilon'/\epsilon)$. The level 3 software was modified for the 1997 run to allow for this effect, resulting in an inefficiency of less than 0.1%. Using $\pi^+\pi^-$ and $\pi^0\pi^0$ data from different running periods does not significantly increase the systematic error on $\mathrm{Re}(\epsilon'/\epsilon)$ because the two modes use essentially independent detector systems; detector inefficiencies and sources of dead time cancel in the K_L/K_S ratio for either mode independently. The only direct effect is a possible difference in the K_S/K_L flux ratio, which will be discussed later.

For off-line selection of $\pi^+\pi^-$ candidates, each pion is required to have a momentum of at least 8 GeV/c and to deposit less than 85% of its energy in the calorimeter. In order to cleanly define the acceptance and to avoid topologies with poor reconstruction efficiency, cuts are made on the distance from each pion to the edges of the drift chambers, calorimeter, MA, and CA, and on the separation distance between the two pions at the drift chambers and calorimeter. The $\pi^+\pi^-$ invariant mass is required to be between 488 and 508 MeV/c^2 (where the mean resolution is approximately 1.6 MeV/c^2) and the square of the transverse momentum of the $\pi^+\pi^-$ system relative to the initial kaon trajectory, p_T^2, is required to be less than 250 MeV$^2/c^2$.

After applying various corrections to the raw calorimeter information, $\pi^0\pi^0$ candidates are reconstructed from four-photon events by choosing the photon pairing combination which is most consistent with the hypothesis of two π^0 decays at a common point, interpreted as the kaon decay vertex. Each photon is required to have an energy of at least 3 GeV and to be at least 5 cm from the outer edge of the CsI and 7.5 cm from any other photon. The four-photon invariant mass is required to be between 490 and 505 MeV/c^2, where the mean mass resolution is approximately 1.5 MeV/c^2. The initial kaon trajectory is unknown, so the only available indicator of kaon scattering is the position of the energy centroid of the four photons at the CsI. This is used to calculate a "ring number," defined as 4 times the square of the larger normal distance (horizontal or vertical), in centimeters, from the energy centroid to the center of the closer beam. Its value is required to be less than 110, which selects events with energy centroid lying within a square region of area 110 cm^2 centered on each beam.

In both the $\pi^+\pi^-$ and $\pi^0\pi^0$ analyses, cuts are made on energy deposits in the MA, photon veto counters, and regenerator. The final samples consist of events with $110 < Z < 158$ m and $40 < E_K < 160$ GeV.

A detailed Monte Carlo (MC) simulation is used to determine the detector acceptance for the $\pi\pi$ signal modes and to evaluate backgrounds. The simulation models kaon production and regeneration to generate decays with the same energy and Z distributions as the data. The decay products are traced through the KTeV detector, allowing for electromagnetic interactions with beam line material and for pion decay. The acceptance is largely determined by the geometry of the detector and by geometric analysis cuts; however, to understand reconstruction biases it is important to simulate the detector response accurately. Energy deposits in the CsI blocks from photons, pions, and electrons are based on the GEANT package [18]. Drift chamber inefficiencies and the delayed-hit effect are simulated using parametrizations and position dependences measured from $\pi^+\pi^-$ data. $\pi e \nu$ and $3\pi^0$ data samples are used to check or tune various aspects of the detector geometry and simulation. To reproduce possible biases due to underlying activity in the detector, an event from the accidental trigger is overlaid on top of each simulated decay; the net effect on the measured value of $\mathrm{Re}(\epsilon'/\epsilon)$ is of order 10^{-4}. MC event samples are subjected to the same reconstruction and selection criteria as the data samples.

Background contributions to the $\pi^+\pi^-$ samples are determined by using sidebands in the mass and p_T^2 distributions to normalize MC predictions for the various background processes. Figures 3(a) and 3(b) show that the p_T^2 distributions for data are well described by the sum of coherent $\pi\pi$ MC and total background MC. $K_L \to \pi e \nu$ and $K_L \to \pi \mu \nu$ decays, with the electron

or muon misidentified as a pion, contribute 0.069% (0.003%) to the vacuum (regenerator) beam. The dominant regenerator-beam background (0.072%) is from kaons which scatter in the regenerator before decaying to $\pi^+\pi^-$. Kaons which scatter in the final beam-defining collimator contribute an additional 0.014% to each beam. Data samples of $\pi^+\pi^-$ decays from kaons which scatter in the regenerator or collimator are used to tune physics-motivated scattering models incorporated into the MC.

The background levels are much larger for the $\pi^0\pi^0$ samples since the ring-number variable is not as effective as p_T^2 at identifying scattered kaons and cannot detect "crossover" scattering from the regenerator into the vacuum beam. Ring-number distributions are shown in Figs. 3(c) and 3(d). The upturn under the peak in Fig. 3(c) is due to $K_L \to 3\pi^0$ decays with lost and/or overlapping photons; it is determined, using mass sidebands, to contribute a background of 0.27% (0.01%) to the vacuum (regenerator) beam. A ring-number sideband (286-792) is used to normalize MC distributions from kaons that scatter before decaying to $\pi^0\pi^0$. The vacuum (regenerator) beam background includes 0.30% (1.07%) from regenerator scattering and 0.16% (0.14%) from collimator scattering. Pairs of π^0's produced by hadronic interactions in the regenerator contribute an additional background of 0.01% in that beam.

After background subtraction, the net yields are 2 607 274 $\pi^+\pi^-$ in the vacuum beam, 4 515 928 $\pi^+\pi^-$ in the regenerator beam, 862 254 $\pi^0\pi^0$ in the vacuum beam, and 1 433 923 $\pi^0\pi^0$ in the regenerator beam.

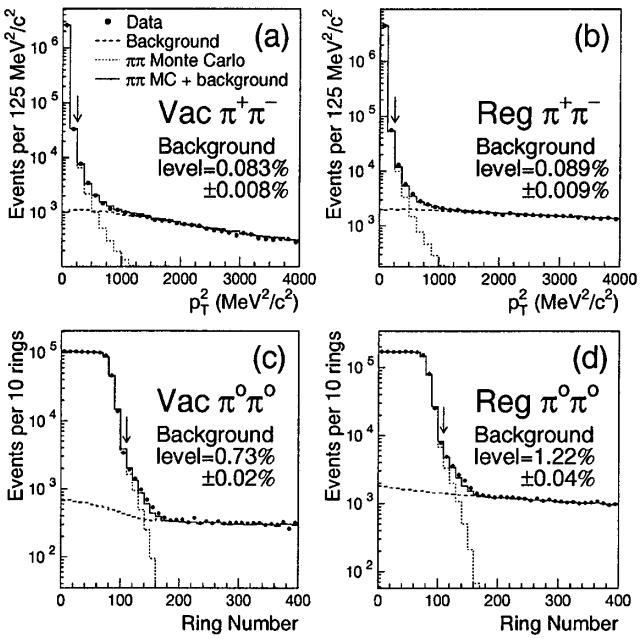

FIG. 3. Distributions of p_T^2 for the $\pi^+\pi^-$ samples and ring number for the $\pi^0\pi^0$ samples. Total background levels and uncertainties (dominated by systematics) are given for the samples passing the analysis cuts (arrows).

$\mathrm{Re}(\epsilon'/\epsilon)$ is extracted from the background-subtracted data using a fitting program which calculates decay vertex distributions, properly treating regeneration and K_S-K_L interference (including the residual K_S component in the vacuum beam at high energy). The acceptance correction (as determined from MC) is applied, and the resulting prediction for each decay mode is integrated over Z and compared to the data in 10-GeV bins of kaon energy. *CPT* symmetry is assumed, and the values of the K_L-K_S mass difference (Δm) and K_S lifetime (τ_S) are fixed to the published average values [19]. The regeneration amplitude is floated in the fit, but constrained to have a power-law dependence on kaon energy, with the phase determined by analyticity [11,20]. The kaon energy distributions are allowed to be different for the $\pi^+\pi^-$ and $\pi^0\pi^0$ modes, with a floating normalization correction in each energy bin for each mode (24 fit parameters). Fitting was done "blind," by hiding the value of $\mathrm{Re}(\epsilon'/\epsilon)$ with an unknown offset, until after the analysis and systematic error evaluation were finalized. The result is $\mathrm{Re}(\epsilon'/\epsilon) = (28.0 \pm 3.0) \times 10^{-4}$, where the error is statistical only. The fit χ^2 is 30 for 21 degrees of freedom.

As a general rule, only biases which affect the K_L and K_S samples differently will lead to systematic errors on $\mathrm{Re}(\epsilon'/\epsilon)$. Possible sources may be divided into four classes: (1) data collection inefficiencies; (2) biases in event reconstruction, sample selection, and background subtraction; (3) misunderstanding of the detector acceptance; and (4) uncertainties in kaon flux and physics parameters. Table I summarizes all of the estimated contributions; only those that are large or require special explanation will be discussed below.

Two large uncertainties in the second class are related to the measurement of photon energies by the calorimeter. A systematic shift in measured energies can shift the reconstructed Z vertex and E_K distributions for the $\pi^0\pi^0$ sample and thus can bias $\mathrm{Re}(\epsilon'/\epsilon)$, mainly by moving K_L events past the fiducial Z cut at 158 m. After calibrating the calorimeter with electrons (and allowing for a small expected electron-photon difference), a final energy scale correction for photons of -0.125% is determined by matching the sharp turn-on of the $\pi^0\pi^0$ Z distribution at the regenerator edge between data and MC. After making this correction, a check using π^0 pairs produced by hadronic interactions in the vacuum window reveals a Z mismatch of 2 cm at the downstream end of the decay region, leading to a systematic error of 0.7×10^{-4} on $\mathrm{Re}(\epsilon'/\epsilon)$. Residual nonlinearities in the calorimeter response, studied from the variation of the mean four-photon invariant mass as a function of E_K, contribute an additional error of 0.6×10^{-4}.

We assign systematic errors based on the dependence of the measured value of $\mathrm{Re}(\epsilon'/\epsilon)$ on variations of key analysis cuts, in particular, the p_T^2 cut for $\pi^+\pi^-$ and the ring-number and photon quality cuts for $\pi^0\pi^0$. No significant dependence on other analysis cuts is observed.

TABLE I. Systematic uncertainties on $\mathrm{Re}(\epsilon'/\epsilon)$.

Source of uncertainty	Uncertainty ($\times 10^{-4}$) From $\pi^+\pi^-$	From $\pi^0\pi^0$
Class 1: Data collection		
Trigger and level 3 filter	0.5	0.3
Class 2: Event reconstruction, selection, backgrounds		
Energy scale	0.1	0.7
Calorimeter nonlinearity	...	0.6
Detector calibration, alignment	0.3	0.4
Analysis cut variations	0.6	0.8
Background subtraction	0.2	0.8
Class 3: Detector acceptance		
Limiting apertures	0.3	0.5
Detector resolution	0.4	<0.1
Drift chamber simulation	0.6	...
Z dependence	1.6	0.7
Monte Carlo statistics	0.5	0.9
Class 4: Kaon flux and physics parameters		
Regenerator-beam attenuation:		
1996 versus 1997	0.2	
Energy dependence	0.2	
Δm, τ_S, regeneration phase	0.2	
Total	2.8	

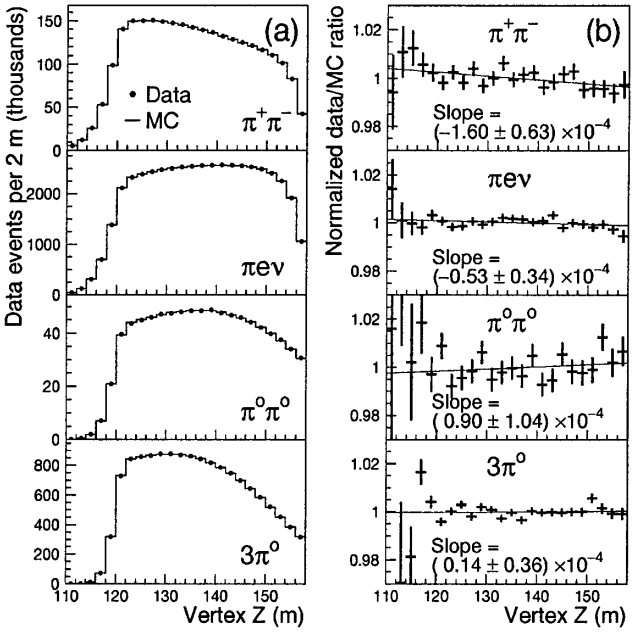

FIG. 4. (a) Data versus Monte Carlo comparisons of vacuum-beam Z distributions for $\pi^+\pi^-$, $\pi e\nu$, $\pi^0\pi^0$, and $3\pi^0$ decays. (b) Linear fits to the data/MC ratio of Z distributions for each of the four samples.

The accuracy of the background determination for the $\pi^0\pi^0$ samples depends on our understanding of kaon scattering in the regenerator and collimator. We consider several variations in the scattering models and in the procedures for tuning the MC with $K \to \pi^+\pi^-$ decays; these affect the shapes of the background MC ring-number distributions, but the sideband normalization procedure limits the impact on $\mathrm{Re}(\epsilon'/\epsilon)$.

The third class of systematic uncertainties, related to detector acceptance, contributes the most to the total systematic error. Many potential detector modeling problems would affect the acceptance as a function of Z, so a crucial check of our understanding of the acceptance is to compare the Z distributions for the data against the MC simulation. Figure 4 shows the vacuum-beam comparisons for the $\pi^+\pi^-$ and $\pi^0\pi^0$ signal modes as well as for the much larger $\pi e\nu$ and $3\pi^0$ samples. The overall agreement is very good, but since the mean Z positions for K_L and K_S decays differ by about 6 m, a relative slope of 10^{-4} per meter in the data/MC ratio would cause an error of 10^{-4} on $\mathrm{Re}(\epsilon'/\epsilon)$. As shown in Fig. 4(b), the $\pi e\nu$ comparison agrees to better than this level; however, the $\pi^+\pi^-$ comparison has a slope of $(-1.60 \pm 0.63) \times 10^{-4}$ per meter. Although the statistical significance of the $\pi^+\pi^-$ slope is marginal, we assign a systematic error on $\mathrm{Re}(\epsilon'/\epsilon)$ based on the full size of the apparent slope, 1.6×10^{-4}. The $3\pi^0$ and $\pi^0\pi^0$ Z distributions agree well, and we place a limit of 0.7×10^{-4} on the possible $\mathrm{Re}(\epsilon'/\epsilon)$ bias from the neutral-mode acceptance.

Other checks on the acceptance include data/MC comparisons of track illuminations at the drift chambers and CsI, photon illumination at the CsI, and minimum photon separation distance. These all agree well and indicate no other sources of acceptance misunderstanding.

The final class of systematic uncertainties includes possible differences in the K_S/K_L flux ratio between the $\pi^+\pi^-$ and $\pi^0\pi^0$ samples. The flux ratio is nominally the same for the 1996 and 1997 running periods because the same regenerator and movable absorber were used; however, we must assign a small uncertainty on $\mathrm{Re}(\epsilon'/\epsilon)$ due to a possible temperature difference which would change their densities and thus the regenerator-beam attenuation. In addition, the $\pi^+\pi^-$ and $\pi^0\pi^0$ samples have somewhat different energy distributions, so the uncertainty in the energy dependence of the attenuation (measured using $\pi^+\pi^-\pi^0$ and $3\pi^0$ data) leads to a small uncertainty on $\mathrm{Re}(\epsilon'/\epsilon)$.

Finally, we assign uncertainties corresponding to one-sigma variations of Δm and τ_S from the published averages [21], and from a deviation of the phase of the regeneration amplitude by $\pm 0.5°$ from the value given by analyticity [20]. Adding all contributions in quadrature, the total systematic uncertainty on $\mathrm{Re}(\epsilon'/\epsilon)$ is 2.8×10^{-4}.

We have performed several cross-checks on the $\mathrm{Re}(\epsilon'/\epsilon)$ result. Consistent values are obtained at all kaon energies, and there is no significant variation as a function of time or beam intensity. Relaxing the power-law constraint on the regeneration amplitude yields a consistent value with the same precision. We have also extracted $\mathrm{Re}(\epsilon'/\epsilon)$ using an alternative fitting technique which compares the vacuum- and regenerator-beam Z distributions directly, eliminating the need for a Monte

Carlo simulation to determine the acceptance. While less statistically powerful, this technique yields a value of $\mathrm{Re}(\epsilon'/\epsilon)$ which is consistent with the standard analysis based on the uncorrelated parts of the statistical and systematic errors. Finally, using $\pi^+\pi^-$ data from 1996 (collected simultaneously with the $\pi^0\pi^0$ data) instead of from 1997 yields a value of $\mathrm{Re}(\epsilon'/\epsilon)$ which is consistent with the standard analysis, allowing a systematic error of 4×10^{-4} due to the 1996 level 3 inefficiency.

In conclusion, we have measured $\mathrm{Re}(\epsilon'/\epsilon)$ to be $[28.0 \pm 3.0(\mathrm{stat}) \pm 2.8(\mathrm{syst})] \times 10^{-4}$; combining the errors in quadrature, $\mathrm{Re}(\epsilon'/\epsilon) = (28.0 \pm 4.1) \times 10^{-4}$. This result definitively establishes the existence of *CP* violation in a decay process, agreeing better with the earlier measurement from NA31 than with E731 [22], and shows that a superweak interaction cannot be the sole source of *CP* violation in the *K* meson system. The average of the three measurements, $(21.7 \pm 3.0) \times 10^{-4}$, while at the high end of standard-model predictions, supports the notion of a nonzero phase in the CKM matrix. Further theoretical and experimental advances are needed before one can say whether or not there are other sources of *CP* violation.

We gratefully acknowledge the support and effort of the Fermilab staff and the technical staffs of the participating institutions for their vital contributions. This work was supported in part by the U.S. Department of Energy, The National Science Foundation, and The Ministry of Education and Science of Japan.

*On leave from C. P. P. Marseille/C. N. R. S., France.

[1] J. H. Christenson, J. W. Cronin, V. L. Fitch, and R. Turlay, Phys. Rev. Lett. **13**, 138 (1964).

[2] For a review, see B. Winstein and L. Wolfenstein, Rev. Mod. Phys. **65**, 1113 (1993).

[3] M. Kobayashi and T. Maskawa, Prog. Theor. Phys. **49**, 652 (1973).

[4] J. Ellis, M. K. Gaillard, and D. V. Nanopoulos, Nucl. Phys. **B109**, 213 (1976); F. J. Gilman and M. B. Wise, Phys. Lett. **83B**, 83 (1979).

[5] M. Ciuchini, Nucl. Phys. (Proc. Suppl.) **59**, 149 (1997).

[6] A. J. Buras, in *Probing the Standard Model of Particle Interactions*, edited by R. Gupta *et al.* (Elsevier, New York, 1999); hep-ph/9806471. This estimate assumes that the mass of the strange quark is $m_s(m_c) = 125 \pm 20\ \mathrm{MeV}/c^2$.

[7] S. Bertolini *et al.*, Nucl. Phys. **B514**, 93 (1998).

[8] L. Wolfenstein, Phys. Rev. Lett. **13**, 562 (1964); Comments Nucl. Part. Phys. **21**, 275 (1994).

[9] L. K. Gibbons *et al.*, Phys. Rev. Lett. **70**, 1203 (1993).

[10] G. D. Barr *et al.*, Phys. Lett. B **317**, 233 (1993).

[11] L. K. Gibbons *et al.*, Phys. Rev. D **55**, 6625 (1997).

[12] V. Bocean *et al.*, Fermilab Report No. TM-2046, 1998 (unpublished).

[13] In contrast, NA31 used a movable K_S target to make the Z distributions similar for K_S and K_L decays, so that the acceptance nearly canceled in the K_S/K_L ratio.

[14] A. Roodman, in *Proceedings of the Seventh International Conference on Calorimetry in High Energy Physics*, edited by E. Cheu *et al.* (World Scientific, Singapore, 1998), p. 89.

[15] J. Whitmore, Nucl. Instrum. Methods Phys. Res., Sect. A **409**, 687 (1998).

[16] These veto elements, primarily the regenerator, cause a dead time of 12% (identical for decays in either beam).

[17] C. Bown *et al.*, Nucl. Instrum. Methods Phys. Res., Sect. A **369**, 248 (1996).

[18] R. Brun *et al.*, computer code GEANT 3.21, CERN, Geneva, 1994. Hadronic interactions are simulated using the FLUKA package.

[19] Particle Data Group, C. Caso *et al.*, Eur. Phys. J. C **3**, 1 (1998).

[20] See R. A. Briere and B. Winstein, Phys. Rev. Lett. **75**, 402 (1995).

[21] If Δm increases by $0.0014 \times 10^{10}\ \hbar\ \mathrm{s}^{-1}$, then $\mathrm{Re}(\epsilon'/\epsilon)$ changes by $+0.05 \times 10^{-4}$. If τ_S increases by 0.0008×10^{-10} s, then $\mathrm{Re}(\epsilon'/\epsilon)$ changes by -0.11×10^{-4}. KTeV will publish new high-precision measurements of Δm and τ_S in the future. Preliminary fits give values which are consistent between the $\pi^+\pi^-$ and $\pi^0\pi^0$ data samples.

[22] Scrutiny of E731 has not revealed any explanation for its lower measured value other than a possible, if improbable, fluctuation.